Estimation of intrathoracic arterial diameter by means of computed tomographic angiography in Hispaniolan Amazon parrots

Hugues Beaufrère, Dr Med Vet; Daniel Rodriguez, MVZ; Romain Pariaut, Dr Med Vet; Lorrie Gaschen DVM, PhD; Rodney Schnellbacher, DVM; Javier G. Nevarez, DVM, PhD; Thomas N. Tully Jr, DVM, MS

Objective—To establish a computed tomography (CT)–angiography protocol and measure the diameters of major arteries in parrots.

Animals—13 Hispaniolan Amazon parrots (*Amazona ventralis*).

Procedures—16-slice CT scanning was used to measure the apparent diameter of the ascending aorta, abdominal aorta, pulmonary arteries, and brachiocephalic trunk. Before scanning, all birds underwent ECG and echocardiographic assessment and were considered free of detectable cardiovascular diseases. Each bird was anesthetized, and a precontrast helical CT scan was performed. Peak aortic enhancement was established with a test bolus technique via dynamic axial CT scan over a predetermined single slice. An additional bolus of contrast medium was then injected, and a helical CT–angiography scan was performed immediately afterward. Arterial diameter measurements were obtained by 2 observers via various windows before and after injection, and intra- and interobserver agreement was assessed.

Results—Reference limits were determined for arterial diameter measurements before and after contrast medium administration in pulmonary, mediastinal, and manual angiography windows. Ratios of vertebral body diameter to keel length were also calculated. Intraobserver agreement was high (concordance correlation coefficients ≥ 0.95); interobserver agreement was medium to high (intraclass correlation coefficients ≥ 0.65).

Conclusions and Clinical Relevance—CT–angiography was safe and is of potential diagnostic value in parrots. We recommend performing the angiography immediately after IV injection of 3 mL of iohexol/kg. Arterial diameter measurements at the described locations were reliable. (*Am J Vet Res* 2011;72:210–218)

Atherosclerosis is a common disease of aging parrots as suggested by results of retrospective pathologic surveys.[1–6] The disease is characterized by the thickening of arterial walls through lipid accumulation and plaque formation in the tunica intima, ultimately resulting in arterial luminal stenosis of the great vessels.[6,7] Atherosclerosis can also lead to arterial aneurysms in pet birds.[8]

Birds are susceptible to diet-induced and spontaneous atherosclerosis.[7] Spontaneous atherosclerosis in pet psittacine birds typically develops in older birds fed a nutritionally unbalanced diet, with risk factors similar to those described for human atherosclerosis.[2,7] Parrots can develop a central form of atherosclerosis, in which the great vessels at the base of the heart are most commonly affected.[2,6,7,9] Antemortem diagnosis of atherosclerosis in these birds has been considered difficult and remains one of the challenges of avian medicine. Only advanced cases of disease with considerable calcification of the great vessels or with secondary heart changes can be diagnosed.[10–13]

Clinical antemortem diagnostic imaging of atherosclerosis in humans includes the use of various modalities of vascular imaging that mainly involve angiographic techniques through the use of high-speed CT

Abbreviations

CI	Confidence interval
CT	Computed tomography
CTA	Computed tomography–angiography
HU	Hounsfield unit
ICC	Intraclass correlation
ROI	Region of interest

Received October 27, 2009.
Accepted January 4, 2010.
From the Department of Veterinary Clinical Sciences, School of Veterinary Medicine, Louisiana State University, Baton Rouge, LA 70803.
Supported by the South Alabama Bird Club, the Gulf South Bird Club, and the Kaytee Avian Foundation.
The authors thank Michael T. Kearney for statistical assistance and Mark Hunter for technical assistance.
Address correspondence to Dr. Beaufrère (hbeaufrere@vetmed.lsu.edu).

scan and magnetic resonance imaging.[14] The main site of arterial stenosis in people is the carotid arteries, and CTA is the principal imaging method to measure carotid diameters and quantify stenosis.[15] Whereas angiography appears to be used in birds, no studies have been conducted to evaluate an angiography protocol in detail and to determine the apparent diameter of intrathoracic arteries in healthy companion birds. The purpose of the study reported here was to establish a CT angiography protocol and provide reference limits for cross-sectional measurements of the great arteries in Hispaniolan Amazon parrots (*Amazona ventralis*).

Materials and Methods

Animals—Thirteen Hispaniolan Amazon parrots were included in the study. Birds were considered healthy on the basis of results of physical examination and a recent CBC. The parrots did not have any clinical signs of cardiovascular disease such as lethargy, anorexia, abdominal distention, or dyspnea prior to the study. They were obtained from a research colony maintained at the Louisiana State University and were fed a pelleted diet.[a] The study protocol was approved by the Louisiana State University Institutional Animal Care and Use Committee.

Cardiological evaluation—All birds were screened for cardiac diseases, with echocardiography performed and ECGs obtained while birds were anesthetized with isoflurane. Echocardiography was performed following the transcoelomic approach,[16–18] with an ultrasonographic probe[b] connected to an ultrasonography system.[c] Morphometric measurements of the left ventricles were obtained with the inner edges method in the vertical view and aortic diameter in the longitudinal view; aortic outflow velocity was measured by use of spectral Doppler technology. All measurements were compared with published reference limits for Amazon parrots.[16–18] The right ventricle was not measured in consideration of its relatively small size in this smaller species of Amazon parrots, lack of detail, and inability to obtain accurate measurements. Electrocardiograms were obtained via an anesthetic monitor,[d] recorded at 100 mm/s with a gain of 10 mm equal to 0.5 mV, and printed via manufacturer software. Measurements were obtained from the recordings and compared with published reference limits for Amazon parrots.[19]

CTA procedures—Each parrot was positioned in dorsal recumbency, and anesthesia was induced via face mask with 5% isoflurane in oxygen at an oxygen flow rate of 0.8 L/min. The parrot was then intubated with an uncuffed endotracheal tube, and anesthesia was maintained with 2% to 3% isoflurane. Supplemental heat was provided by a heating pad and forced warm air.[e] A 24- or 26-gauge catheter[f] was placed in the left ulnar vein (n = 10 parrots), right ulnar vein (2), or medial metatarsal vein (1). An injection plug[g] was placed at the end of the catheter, and the catheter was secured in place with an adhesive bandage.[h] A 1-mL syringe containing the contrast medium was connected to the catheter by a 22-gauge butterfly catheter.[i]

The CTA examinations were performed with a 16-detector-row CT scanner.[j] Whole-body scout scans were performed in orthogonal planes. A survey examination was performed before contrast medium administration (precontrast) by use of a built-in abdominal scan protocol with the following parameters: standard algorithm in helical scan mode, 1.25-mm slice thickness, 1.375 pitch, 100 kVp, and 150 mA. The scan area of interest extended from the last cervical vertebra just cranial to the coracoid bone and continued caudally to the coxofemoral joint. A dynamic CT scan was performed at the level of the abdominal aorta dorsal to the proventriculus and began 3 seconds before an initial manual bolus injection of iohexol[k] (1 mL/kg), which was administered over 1 second. The person manually injecting the contrast medium was positioned behind a mobile lead x-ray shield.

When precontrast survey scans were completed, CTA was performed with the same scan parameters but with a manual injection of 3 mL of iohexol/kg over 3 seconds, administered 3 seconds prior to initiation of CTA. Additional reconstruction series at 0.625 mm and bone algorithm were performed. Dynamic scans allowed time of arrival of contrast medium to the abdominal aorta (time to enhancement peak) to be determined.

ROI measurements—The attenuation coefficient (in HU) was obtained for each vessel including the 2 brachiocephalic trunks, the aorta, and the 2 pulmonary arteries to quantify the amount of contrast medium present in these arteries. Circular ROIs corresponding to the cross-sectional area of all the major arteries before and after contrast administration were obtained. The circular measurement tool gave the area of the ROI from which the diameter (D) was calculated with the following formula:

$$D = 2(\text{area}/\pi)^{1/2}$$

A pulmonary window (width, 1,400 HU; level, –500 HU) was used for pre- and postcontrast measurements (**Figure 1**). Additional windows used for ROI measurements made after contrast agent administration (postcontrast) included a mediastinal window (width, 350; level, 50) and an angiography window, with the window level determined from the mean contrast attenuation coefficient in the 6 measured arteries and the window width determined by calculating the following ratio: window width/window level = 2. The ratio used was derived from the following formula:

$$W/AC = (3.3 \times L/AC) - 1.3$$

in which W is the window width, AC is the attenuation coefficient, and L is the window level used (L = mean AC of vessels for this protocol). This formula was obtained from a previously reported CTA study[20] on phantom arteries of various sizes, which was conducted to determine optimum CT levels and windows.

Regions of interest were obtained as the largest circle that would encompass the outermost outline of the arteries before contrast medium administration and the outermost outline of the contrast boundary after administration (**Figure 2**). For precontrast measurements, the unsharp edges of the arteries were in-

cluded in the measurements, whereas for postcontrast measurements, such edges were not included to obtain luminal diameters and minimize inaccuracy due to blooming and penumbra artifacts caused by the contrast medium and algorithm used, respectively. The left and right brachiocephalic trunks were measured at the same level as they laterally crossed the cranial thoracic cavity. The ascending aorta was measured at the middle of its ascending course. The abdominal aorta was measured prior to the bifurcation of the mesenteric artery. The left and right pulmonary arteries were measured at the middle of their ascending course to the lungs.

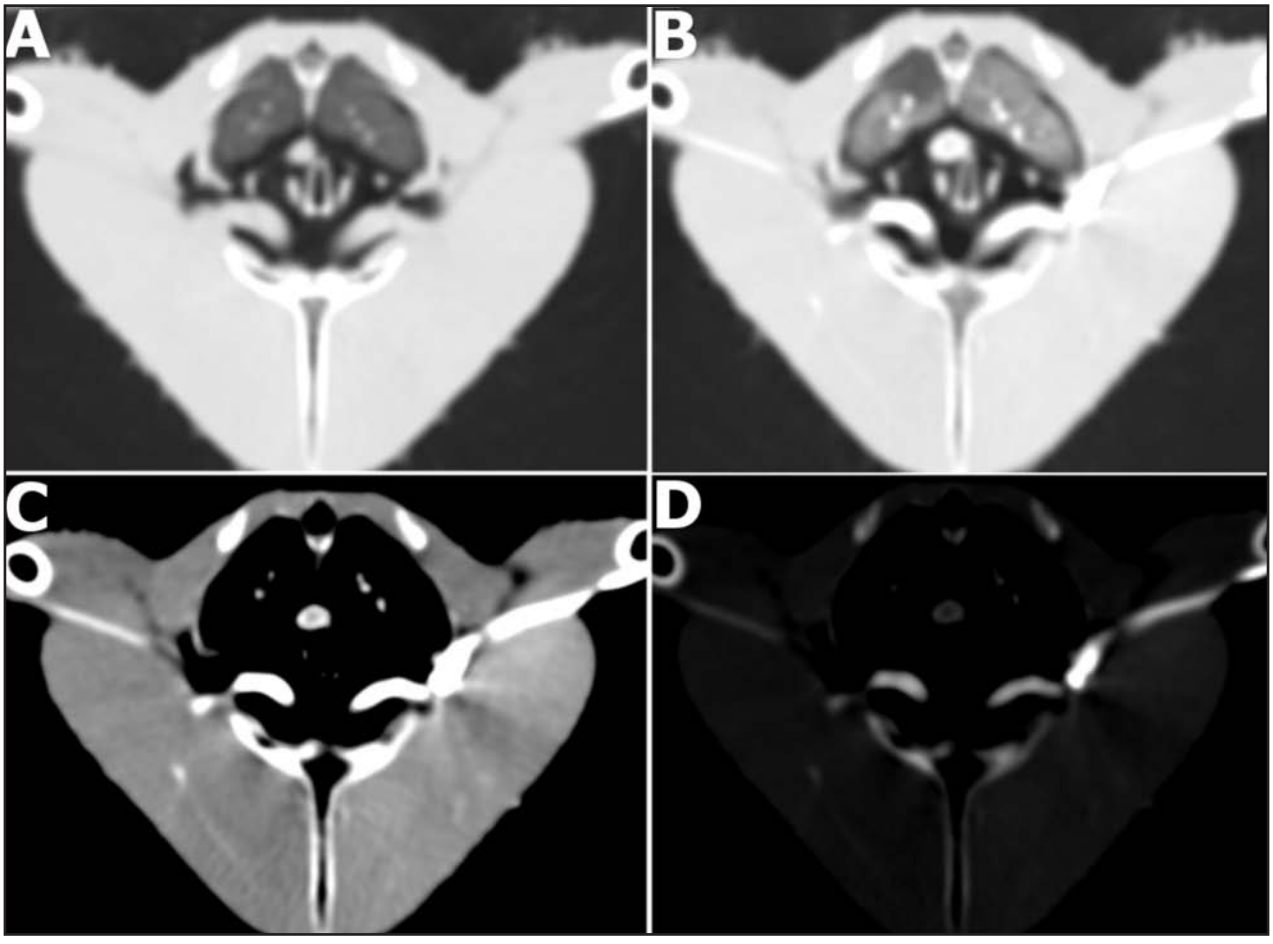

Figure 1—Computed tomography–angiography scan of a healthy Hispaniolan Amazon parrot obtained at the level of the brachiocephalic trunks in a pulmonary window (A) before contrast medium administration and in a pulmonary window (B), mediastinal window (C), and manually selected angiography window (D) after administration.

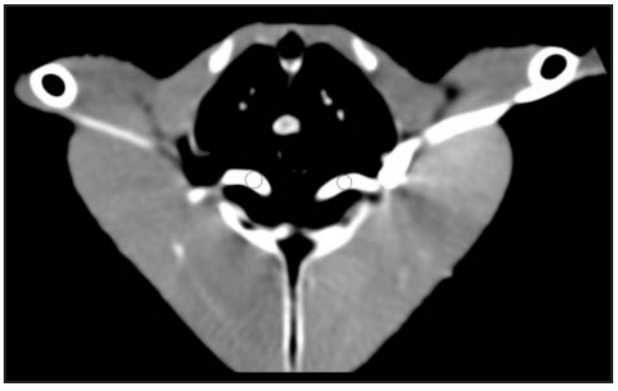

Figure 2—Computed tomography–angiography scan of a Hispaniolan Amazon parrot obtained at the level of the brachiocephalic trunks in a mediastinal window. Circular ROIs (circles) were used to measure the diameters of the right and left brachiocephalic trunks.

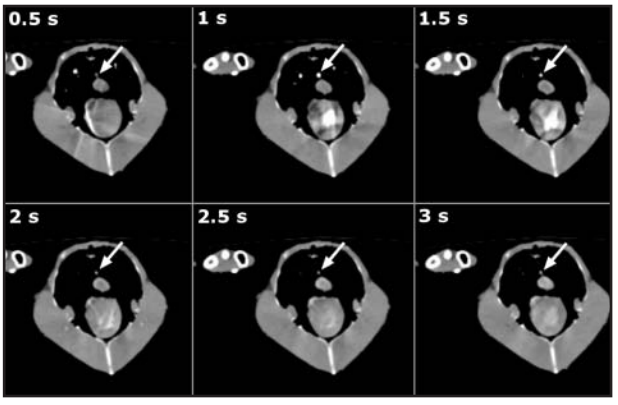

Figure 3—Dynamic axial CTA scan of a Hispaniolan Amazon parrot obtained at the level of the abdominal aorta at various points after administration of contrast medium. The contrast enhancement of the abdominal aorta (arrows) is seen over time with the enhancement peak at 1 second.

Ratios were also calculated with the length of the keel bone and length of the vertebral body at the coracoid-keel junction as obtained via a bone window.

Two observers participated in ROI measurements. Observer 1 (the radiologist) obtained all measurements twice on different days to evaluate intraobserver agreement (reproducibility) of the measurement techniques. Additionally, observer 2 (the clinician) obtained measurements to evaluate interobserver agreement. Outlining of ROIs, linear measurements, and 3-D reconstruction (segmentation and volume rendering) of the heart and great vessels were performed with a commonly used and calibrated imaging program.[l] Cross-sectional images were magnified at 300% to improve accuracy of measurements.

Statistical analysis—Analyses were performed by use of the same computer software,[m] except where indicated. Data were tested for normality with a Shapiro-Wilk test, with a value of $P < 0.05$ indicating a nonnormal distribution. Results are reported as mean ± SD when the data were normally distributed and as median (range) when they were not. Univariate summary statistics were calculated to report echocardiographic measurements, CT artery diameters, and ratios. Reference limits were determined as the central 95% of the values (ie, the mean ± 2 SD) for normally distributed data and the interval between the 2.5th and 97.5th percentiles for nonnormally distributed data.

For CTA measurements, with measurements of the various arteries considered dependent variables, differences between the means of these measurements with and without contrast medium administration, with the various CT windows, and between observers were assessed by means of ANOVA on the ranked value blocked for individual birds. Multiple post hoc comparisons were performed with the Tukey and the least squares means methods. The Wilcoxon matched-pairs signed rank test was used to assess differences between the means of the diameters of the 2 brachiocephalic trunks, the 2 pulmonary arteries, and the 2 consecutive measurements by the same observer (the radiologist).

Spearman rank correlation coefficients (ρ) were calculated to assess the correlation between the sizes of the various arteries and with the parrot body weight overall and for each CT window. A correlation was considered strong when the coefficient was > 0.5 and weak when ≤ 0.5. Intraobserver agreement (reproducibility) between 2 consecutive measurements was evaluated by calculating concordance correlation coefficients for each artery.[21] Reproducibility was considered high when the coefficient value was ≥ 0.76, medium when between 0.40 and 0.75, and low when ≤ 0.39. Interobserver agreement between the radiologist and clinician was evaluated by calculating ICC coefficients.[22,n] The 2-way, random, single-measure reliability ICC for absolute agreement and 95%

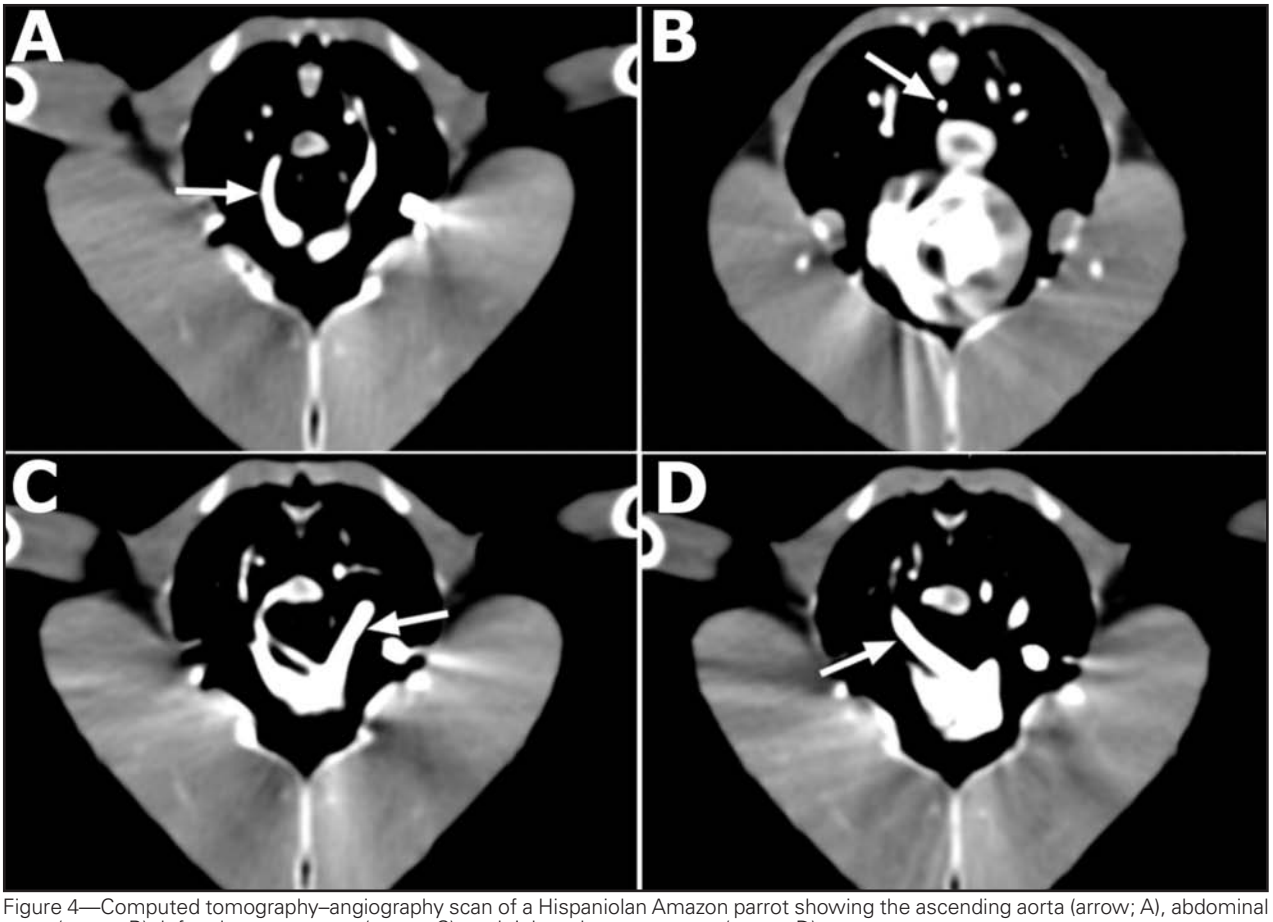

Figure 4—Computed tomography–angiography scan of a Hispaniolan Amazon parrot showing the ascending aorta (arrow; A), abdominal aorta (arrow; B), left pulmonary artery (arrow; C), and right pulmonary artery (arrow; D).

CIs were determined for each artery. Interobserver agreement was considered high when the coefficient value was ≥ 0.76, medium when between 0.40 and 0.75, and low when ≤ 0.39. Values of $P < 0.05$ were considered significant for all analyses.

Results

Cardiological evaluation—The 13 Hispaniolan Amazon parrots had a mean ± SD body weight of 290.5 ± 21.2 g. No cardiac abnormalities were detected nor were any clinically important arrhythmias identified on ECGs. All ECG measurements were within reference limits reported for Amazon parrots.[19] No echocardiographic reference limits are available for the *A ventralis*, which is a smaller species of the genus *Amazona*, so published reference limits were used for the genus *Amazona*, which were obtained from 4 larger species of Amazon parrots (*Amazona amazonica*, *Amazona aestiva*, *Amazona ochrocephala*, and *Amazona viridigenalis*).[18] Compared with those reference limits, some echocardiographic measurements (left ventricular width in diastole, left ventricular width in systole, and left ventricular length in systole) were slightly lower. No abnormalities in cardiac shape and function were detected via echocardiography. Therefore, on the basis of aforementioned results, the 13 parrots were considered free of detectable cardiovascular diseases.

Mean ± SD echocardiographic measurements were as follows: left ventricular width in diastole, 5.60 ± 1.21 mm; left ventricular length in diastole, 20.1 ± 2.46 mm; left ventricular width in systole, 4.22 ± 0.93 mm; left ventricular length in systole, 18.26 ± 2.82 mm; aortic root diameter, 3.35 ± 0.39 mm; aortic outflow velocity, 75.46 ± 15.75 cm/s; left ventricular width-to-length ratio in diastole, 0.28 ± 0.08; left ventricular width-to-length ratio in systole, 0.23 ± 0.05; and left ventricular fractional shortening, 24.03 ± 12.79%.

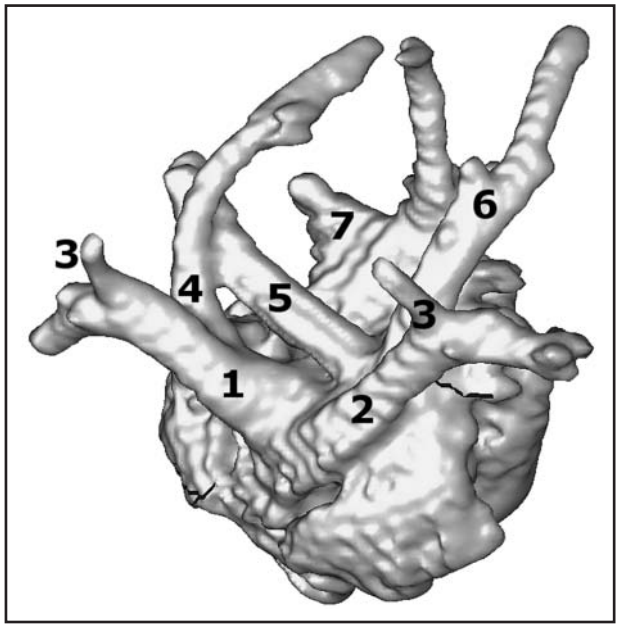

Figure 5—Diagram of the 3-D segmentation of the heart of a Hispaniolan Amazon parrot as obtained via segmentation and volume rendering techniques made possible by CTA. The image is oriented to display a cranial view of the base. 1 = Right brachiocephalic trunk. 2 = Left brachiocephalic trunk. 3 = Carotid arteries. 4 = Ascending aorta. 5 = Right pulmonary artery. 6 = Left pulmonary artery. 7 = Pulmonary veins.

CTA—With the dynamic axial CT, the enhancement peak in the abdominal aorta ranged from 0.5 to 2 seconds after contrast medium administration (**Figure 3**). The CTA scans obtained through helical CT acquisition were of good quality and diagnostic value. The mean ± SD attenuation coefficients of the left and right brachiocephalic trunks, the ascending aorta, and the abdominal aorta were 366 ± 129 HU, 404 ± 193 HU, 332 ± 101 HU, and 253 ± 123 HU, respectively. Median (range) attenuation coefficients in the left and right pulmonary arteries were 260 (89 to 849) HU and 259 (103 to 847) HU, respectively. For comparison, the attenuation coefficient of soft tissue is 20 to 50 HU.

Administration of contrast medium considerably enhanced visualization of the major arteries in various window settings (Figures 1 and 4), particularly the smaller diameter arteries such as the carotid arteries and the abdominal aorta. Three-dimensional reconstruction of the heart and central vasculature by means of segmentation and volume rendering techniques was also possible with CTA (**Figure 5**). No adverse effects were observed in the parrots during or after contrast administration.

ROI measurements—All arterial diameters were considered as apparent arterial diameters because of the lack of gold standard for arterial diameter measurements in birds and the likelihood of motion artifacts. All measurements made before and after contrast medium administration at the various window settings (pulmonary, mediastinal, and angiography) were normally distributed with the exception of the measurements of the left brachiocephalic trunk via the angiography window. Reference limits for the length of the 6 measured arteries were summarized (**Table 1**). For these arteries, there were significant (all $P < 0.005$) differences between the means of arterial measurements made before (precontrast) and after (postcontrast) contrast medium administration and via the various windows. In descending order, the largest apparent arterial diameters were observed precontrast, postcontrast via the pulmonary window, postcontrast via the mediastinal window, and postcontrast via the angiography window.

Ratios between the diameters of the major arteries with the keel length and with the vertebral body length were also determined (**Tables 2 and 3**). For the 13 parrots, internal marker lengths were normally distributed and were 24.6 ± 0.5 mm for the keel and 4.6 ± 0.3 mm for the vertebral body. When the effects of contrast medium administration and window settings were not considered, there was no significant ($P = 0.219$) difference between the diameters of the left and right pulmonary arteries but there was a significant ($P < 0.001$) difference between the diameters of the left and right brachiocephalic trunks, with the right being larger. When controlling for the effect of contrast medium administration and window settings, there was no difference between the left and right pulmonary arteries (all $P > 0.096$). There was also no difference between the diameters of the left and right brachiocephalic trunks

Table 1—Reference limits for apparent diameters (mm) of the major arteries of 13 healthy Hispaniolan Amazon parrots as measured via CTA before and after contrast medium administration and via various windows.

	Pulmonary window				Mediastinal window		Angiography window	
Artery	Precontrast value	Reference limits	Postcontrast value	Reference limits	Postcontrast value	Reference limits	Postcontrast value	Reference limits
LB	3.2 ± 0.3	2.5–3.8	2.7 ± 0.4	2.0–3.5	2.4 ± 0.3	1.8–3.1	2*	1.7–2.9
RB	3.5 ± 0.3	3.0–4.0	2.9 ± 0.4	2.1–3.6	2.5 ± 0.3	1.8–3.1	2.2 ± 0.3	1.5–2.7
AO	2.5 ± 0.2	2.0–2.9	2.2 ± 0.4	1.3–3.4	1.9 ± 0.3	1.3–2.5	1.7 ± 0.3	0.9–2.3
AA	2.3 ± 0.2	1.8–2.7	1.9 ± 0.3	1.4–2.5	1.5 ± 0.4	0.8–2.2	1.3 ± 0.1	1.0–1.6
LP	2.5 ± 0.3	1.7–3.2	2.4 ± 0.3	1.8–3.0	1.9 ± 0.2	1.4–2.3	1.6 ± 0.3	1.0–2.1
RP	2.3 ± 0.3	1.7–2.9	2.4 ± 0.2	2.0–2.8	1.9 ± 0.3	1.3–2.5	1.6 ± 0.4	0.9–2.3

Pre- and postcontrast values are reported as mean ± SD unless otherwise indicated.
*Data for this circumstance were not normally distributed; therefore, median is reported.
AA = Abdominal aorta. AO = Ascending aorta. LB = Left brachiocephalic trunk. LP = Left pulmonary artery. RB = Right brachiocephalic trunk. RP = Right pulmonary artery.
Reference intervals for normally distributed data were calculated as mean ± 2 SD. Intervals for nonnormally distributed data represent the 2.5th and 97.5th percentiles. Reference limits may not exactly equal mean ± 2 SD because of rounding.

Table 2—Reference limits for keel-to-apparent arterial diameter ratio of the major arteries of 13 healthy Hispaniolan Amazon parrots as measured via CTA before and after contrast medium administration and via various windows.

	Pulmonary window				Mediastinal window		Angiography window	
Ratio	Precontrast value	Reference limits	Postcontrast value	Reference limits	Postcontrast value	Reference limits	Postcontrast value	Reference limits
LB:KL	0.13 ± 0.01	0.10–0.16	0.11 ± 0.02	0.08–0.14	0.10 ± 0.01	0.07–0.13	0.08*	0.07–0.12
RB:KL	0.14*	0.13–0.17	0.08 ± 0.15	0.08–0.15	0.07 ± 0.13	0.07–0.13	0.08*	0.07–0.11
AO:KL	0.10*	0.08–0.11	0.05 ± 0.12	0.05–0.12	0.05 ± 0.10	0.05–0.10	0.07 ± 0.01	0.04–0.09
AA:KL	0.09*	0.08–0.10	0.08*	0.06–0.09	0.06*	0.04–0.08	0.06*	0.04–0.06
LP:KL	0.10 ± 0.02	0.06–0.13	0.10 ± 0.01	0.07–0.12	0.07*	0.07–0.09	0.06 ± 0.01	0.04–0.09
RP:KL	0.10 ± 0.01	0.07–0.12	0.10 ± 0.01	0.07–0.12	0.08 ± 0.01	0.05–0.10	0.07 ± 0.01	0.04–0.09

KL = Keel length.
See Table 1 for remainder of key.

Table 3—Reference limits for vertebral body-to-apparent arterial diameter ratio of the major arteries of 13 healthy Hispaniolan Amazon parrots as measured via CTA before and after contrast medium administration and via various windows.

	Pulmonary window				Mediastinal window		Angiography window	
Ratio	Precontrast value	Reference limits	Postcontrast value	Reference limits	Postcontrast value	Reference limits	Postcontrast value	Reference limits
LBL:VL	0.67 ± 0.07	0.53–0.82	0.58 ± 0.09	0.40–0.76	0.52 ± 0.07	0.37–0.66	0.41*	0.36–0.63
RBL:VL	0.75 ± 0.07	0.60–0.90	0.61 ± 0.08	0.44–0.78	0.53 ± 0.08	0.37–0.68	0.46 ± 0.07	0.32–0.61
AOL:VL	0.52 ± 0.06	0.41–0.64	0.47 ± 0.09	0.28–0.66	0.40 ± 0.07	0.25–0.55	0.35 ± 0.08	0.19–0.50
AAL:VL	0.49 ± 0.05	0.40–0.58	0.42 ± 0.06	0.30–0.54	0.33 ± 0.08	0.16–0.49	0.27 ± 0.04	0.20–0.35
LPL:VL	0.50 ± 0.07	0.37–0.68	0.51 ± 0.07	0.35–0.68	0.41 ± 0.06	0.30–0.49	0.35 ± 0.06	0.22–0.46
RPL:VL	0.49*	0.42–0.67	0.51 ± 0.07	0.36–0.65	0.41 ± 0.06	0.28–0.53	0.35 ± 0.06	0.22–0.48

AAL = Abdominal aorta length. AOL = Ascending aorta length. LBL = Left brachiocephalic trunk length. LPL = Left pulmonary artery length. RBL = Right brachiocephalic trunk length. RPL = Right pulmonary artery length. VL = Vertebral body length.
See Table 1 for remainder of key.

(all $P > 0.088$) except for the precontrast diameter values, with values for the right being significantly ($P = 0.002$) larger than for the left.

Body weight was not correlated with diameter of the major arteries overall and within window settings (all $P > 0.05$). However, when the presence of contrast medium and the window settings were not taken into account, strong associations were detected between the diameters of the major arteries (all $P < 0.001$; all $\rho > 0.65$). When considering the presence of contrast medium and the window settings, there was a strong correlation between the diameters of the 2 brachiocephalic trunks and between both brachiocephalic trunks and the ascending aorta in the pulmonary ($P < 0.014$; $\rho > 0.66$) and mediastinal windows ($P < 0.023$; $\rho > 0.62$) and only between the diameters of the 2 brachiocephalic trunks but not between both brachiocephalic trunks and the ascending aorta in the precontrast ($P = 0.029$; $\rho = 0.6$) and angiography ($P = 0.007$; $\rho = 0.7$) windows. The diameters of the left and right pulmonary arteries were strongly correlated in all settings except the mediastinal window ($P < 0.037$; $\rho > 0.6$). Correlation patterns were similar for the calculated ratios.

Table 4—Intraobserver agreement (reproducibility) for a clinician and interobserver agreement between a radiologist and clinician for arterial CTA measurements in 13 Hispaniolan Amazon parrots.

	CCC		ICC (2,1)		
Artery	Correlation	95% CI	Correlation	95% CI	*P* value
LB	0.98	0.97–0.99	0.75	0.58–0.86	< 0.001
RB	0.99	0.98–0.99	0.89	0.81–0.93	< 0.001
AO	0.96	0.93–0.98	0.76	0.62–0.86	< 0.001
AA	0.95	0.93–0.98	0.84	0.73–0.90	< 0.001
LP	0.97	0.95–0.99	0.65	0.46–0.78	< 0.001
RP	0.99	0.98–1.00	0.72	0.56–0.83	< 0.001

CCC = Concordance correlation coefficient for 2 measurements made by 1 individual. ICC (2,1) = 2-way, random, single-measure reliability ICC coefficient for absolute agreement comparing the clinician's measurements with those of the radiologist.
See Table 1 for remainder of key.

The means of measurements made by 2 observers (the radiologist and clinician) did not differ significantly (all $P > 0.072$), except for those of the left brachiocephalic trunk ($P = 0.047$) in which the clinician had larger values than the radiologist. Similarly, no significant (all $P > 0.588$) differences were evident between the means of 2 consecutive measurements by the same observer (the radiologist).

Intraobserver agreement (reproducibility) was high, with all concordance correlation coefficients > 0.95 (**Table 4**). Interobserver agreement was high for measuring diameters of the brachiocephalic trunks, the ascending aorta, and the abdominal aorta and was medium for the pulmonary arteries. Results of the reliability assessment were similar for the calculated ratios.

Discussion

In the study reported here, a protocol for CTA and reference limits for apparent luminal arterial diameters and ratios were developed for Hispaniolan Amazon parrots. On the basis of our findings, we recommend performing a dynamic axial CT with a test bolus consisting of 25% of the total contrast medium dose (ie, 1 mL/kg of a total dose of 4 mL/kg) to ensure the catheter is correctly located and determine the time delay to be used during angiographic scanning. A helical CT angiography scan can then be performed with the time delay obtained from the previous test bolus technique, and the remaining dose of contrast medium (ie, 75% or 3 mL/kg) can be administered. We chose manual injections rather than an automated injection synchronized with the CT machine because of poor results obtained with previous attempts, which were probably attributable to the small injection volume and the 3-second delay between activation of the pump and the start of the scan.

The CTA method described here appears safe and of potential diagnostic value as demonstrated by the adequate amount of contrast present in the major arteries. Although adequate visualization of the major arteries was obtained with nonenhanced CT, in particular for the brachiocephalic trunks with a pulmonary or bone window, visualization was greatly improved with the angiography procedure in several window settings. Furthermore, CTA allowed evaluation of smaller diameter arteries, assessment and measurement of the apparent arterial lumens, and 3-D reconstruction and segmentation of the heart and central vasculature, thereby enhancing its diagnostic value.

The interval to enhancement peak in the aorta was fast and just a few seconds from the initiation of contrast medium administration. This interval is considerably longer in humans and dogs, with means varying between 25 to 45 seconds.[23,24] It depends on many factors such as the type of contrast medium and the duration and rate of injection.[23,24] However, considering the fast circulation of contrast medium in the avian vascular system, it would be difficult to confirm the influence of any of these factors.

Arterial measurements were window-dependent in the present study; therefore, we recommend using window-specific reference limits when evaluating the apparent luminal diameter of the major arteries in Hispaniolan Amazon parrots. We recommend measuring the arteries via a mediastinal or angiography window, which eliminates penumbra and blooming (blurring) of the arteries and provides better delineation of the contrast medium. Overall, the diameters of the brachiocephalic trunks and pulmonary arteries on one side were not significantly different than those on the other side, and there was a positive correlation between the arterial diameters of both sides. Use of ratios may prove beneficial in the extrapolation of these results to psittacine species of various sizes, particularly other Amazon parrot species. The measurement method involving circular ROI measurements at the described arterial locations had medium to high reliability as suggested by high intra-observer agreement and medium to high interobserver agreement.

The accuracy of CTA is considerably affected by the attenuation coefficient of contrast material within the vessel, the window settings used for measurement, and the arterial inner diameter.[20,25,26] Several studies have involved use of vascular models (phantoms) to determine the most accurate settings for measuring arterial luminal diameters and subsequently quantifying degrees of arterial stenosis. For example, the angiography window formula used in our study yielded the most accurate CTA measurements on phantom arteries of various diameters.[20] In another phantom study,[25] results suggested that measurement inaccuracy increases with attenuation coefficients < 150 or > 250 HU. However, a different phantom study[26] involving automated software revealed that measurement errors decrease as densities of intravascular contrast medium increase, with the least measurement error obtained when a high-density vascular model of 460 HU is used. In the study reported here, attenuation coefficients for the arteries after contrast administration were high (overall mean ± SD, 333 ± 167 HU). The fast heart rate and circulation of contrast medium in the vascular system of birds might limit the ability to obtain a predetermined attenuation coefficient in the selected arteries. Moreover, greater contrast enhancement may be needed to adequately visualize the small arteries of psittacine species.

Our study has some limitations. First, the major arteries at the base of the heart move with heart beat, which may induce considerable motion artifacts during sequence acquisition, possibly decreasing accuracy of

the diameter measurements. Changes in arterial diameters and positions likely occur during the cardiac cycle and could potentially lead to differences in measurements performed in the present study. In addition, the small size of the study birds limited visualization of the smaller arteries such as the carotid arteries cranially, the mesenteric artery, and other branches of the brachial arteries and the abdominal aorta. Furthermore, all manual measurements involved some degree of subjectivity. Automated software for CTA is available and may provide more objectivity in arterial measurements. Its usefulness has been investigated in a phantom study.[26] Finally, the reference limits created through our study have not been evaluated in diseased birds; therefore, the potential of CTA in the diagnosis of vascular conditions remains unknown.

Several case reports of birds with central atherosclerosis have described the presence of stenosis or narrowing of arterial lumens. A substantial luminal narrowing (approx 50%) of the ascending aorta and pulmonary arteries was detected through gross examination and histologic analysis in an African grey parrot.[12] A blue and gold macaw that was suspected to have narrowing of the aorta and brachiocephalic arteries on angiography was found at necropsy to have narrowed arterial lumens.[11] A blue-fronted Amazon parrot was also found to have a 60% to 95% reduction in lumen diameter of the carotid arteries caused by atherosclerosis.[27] Furthermore, several examples of arterial luminal stenosis are cited in reviews on atherosclerosis in birds.[7,28] These reports support CTA as potentially useful in the evaluation of birds with suspected vascular stenosis. Additionally, a phantom study[26] of the effect of vascular inner diameter on measurement accuracy showed similar measurement errors existed among the 3-, 4-, and 6-mm-diameter vascular models through use of a standard algorithm. The results of the present study suggested that CTA may be of value in assessing the major arteries of psittacine species that are of sizes similar to the small vascular models. However, given the small size of the species evaluated, it is possible that arterial lumens cannot be measured accurately and that quantification of the amount of stenosis may not be achievable. To further determine the accuracy of CTA measurements in birds, such measurements will need to be confirmed at necropsy on healthy birds and birds with cardiovascular diseases, including atherosclerosis.

Arterial luminal stenosis is a consequence of atherosclerosis in psittacine birds and is believed to be a contributing factor to clinical signs, tissue ischemia, or acute death in affected birds. However, the degree and clinical importance of arterial luminal stenosis has not been properly characterized. More studies are needed to investigate the relationship between arterial stenosis, atherosclerosis, and clinical signs of disease in birds. Studies are also needed to establish and improve the potential of CTA in the diagnosis of atherosclerosis in parrots.

a. Kaytee Exact Rainbow, Chilton, Wis.
b. S12-4 Sector Array Transducer, Philips Healthcare, Andover, Mass.
c. IE 33, Philips Healthcare, Andover, Mass.
d. Vetspecs VMS7, VetSpecs Inc, Canton, Ga.
e. Bair Hugger, Arizant Inc, Prairie, Minn.
f. Abdocath-T, Hospira Venisystems, Sligo, Ireland.
g. Surflo Injection Plug, Terumo Medical Products, Somerset, NJ.
h. Tegaderm, 3M, Saint Paul, Minn.
i. Vacutainer Safety-Lok blood collection set, Becton Dickinson, Franklin Lakes, NJ.
j. Light Speed GE Healthcare, Milwaukee, Wis.
k. Omnipaque 240 mg/mL, GE Healthcare Inc, Princeton, NJ.
l. OsiriX Imaging Software, version 3.5.1, OsiriX Foundation, Geneva, Switzerland. Available at: www.osirix-viewer.com. Accessed Jun 1, 2009.
m. SAS, version 9.1.3, SAS Institute Inc, Cary, NC.
n. SPSS, version 16.0, SPSS Inc, Chicago, Ill.

References

1. Braun S, Krautwald-Junghanns ME, Straub J. About type and incidence of heart disease in psittacines kept in captivity in Germany [in German]. *Dtsch Tierarztl Wochenschr* 2002;109:255–260.
2. Krautwald-Junghanns ME, Braun S, Pees M, et al. Research on the anatomy and pathology of the psittacine heart. *J Avian Med Surg* 2004;18:2–11.
3. Bohorquez F, Stout C. Aortic atherosclerosis in exotic avians. *Exp Mol Pathol* 1972;46:11–19.
4. Pilny AA. Retrospective of atherosclerosis in psittacine birds: clinical and histopathologic findings in 31 cases, in *Proceedings*. Assoc Avian Vet Conf 2004;349–351.
5. Garner MM, Raymond JT. A retrospective study of atherosclerosis in birds, in *Proceedings*. Assoc Avian Vet Conf 2003;59–66.
6. Fricke C, Schmidt V, Cramer K, et al. Characterization of atherosclerosis by histochemical and immunohistochemical methods in African Grey parrots (*Psittacus erithacus*) and Amazon parrots (*Amazona* spp.). *Avian Dis* 2009;53:466–472.
7. Bavelaar FJ, Beynen AC. Atherosclerosis in parrots. A review. *Vet Q* 2004;26:50–60.
8. Vink-Nooteboom M, Schoemaker NJ, Kik MJ, et al. Clinical diagnosis of aneurysm of the right coronary artery in a white cockatoo (*Cacatua alba*). *J Small Anim Pract* 1998;39:533–537.
9. Oglesbee BL, Oglesbee MJ. Results of postmortem examination of psittacine birds with cardiac disease: 26 cases (1991–1995). *J Am Vet Med Assoc* 1998;212:1737–1742.
10. Mans C, Brown CJ. Radiographic evidence of atherosclerosis of the descending aorta in a grey-cheeked parakeet (*Brotogeris pyrrhopterus*). *J Avian Med Surg* 2007;21:56–62.
11. Phalen DN, Hays HB, Filippich LJ, et al. Heart failure in a macaw with atherosclerosis of the aorta and brachiocephalic arteries. *J Am Vet Med Assoc* 1996;209:1435–1440.
12. Sedacca CD, Campbell TW, Bright JM, et al. Chronic cor pulmonale secondary to pulmonary atherosclerosis in an African Grey parrot. *J Am Vet Med Assoc* 2009;234:1055–1059.
13. Shrubsole-Cockwill A, Wojnarowicz C, Parker D. Atherosclerosis and ischemic cardiomyopathy in a captive, adult red-tailed hawk (*Buteo jamaicensis*). *Avian Dis* 2008;52:537–539.
14. Sanz J, Fayad ZA. Imaging of atherosclerotic cardiovascular disease. *Nature* 2008;451:953–957.
15. Bartlett ES, Walters TD, Symons SP. Carotid stenosis index revisited with direct CT angiography measurement of carotid arteries to quantify carotid stenosis. *Stroke* 2007;38:286–291.
16. Pees M, Krautwald-Junghanns ME. Avian echocardiography. *Sem Avian Exotic Pet* 2005;14:14–21.
17. Pees M, Krautwald-Junghanns ME, Straub J. Evaluating and treating the cardiovascular system. In: Harrison GJ, Lightfoot TL, eds. *Clinical avian medicine*. Palm Beach, Fla: Spix Publishing, 2006;379–394.
18. Pees M, Straub J, Krautwald-Junghanns ME. Echocardiographic examinations of 60 African Grey parrots and 30 other psittacine birds. *Vet Rec* 2004;155:73–76.
19. Nap AM, Lumeij JT, Stokhof AA. Electrocardiogram of the African Grey (*Psittacus erithacus*) and Amazon (*Amazona* spp.) parrot. *Avian Pathol* 1992;21:45–53.
20. Liu Y, Hopper KD, Mauger DT, et al. CT angiography measurement of the carotid artery: optimizing visualization by manipu-

lating window and level settings and contrast material attenuation. *Radiology* 2000;217:494–500.
21. Lin LI-K. A concordance correlation coefficient to evaluate reproducibility. *Biometrics* 1989;45:255–268.
22. Shrout PE, Fleiss JL. Intraclass correlations: uses in assessing rater reliability. *Psychol Bull* 1979;86:420–428.
23. Awai K, Hiraishi K, Hori S. Effect of contrast material injection duration and rate on aortic peak time and peak enhancement at dynamic CT involving injection protocol with dose tailored to patient weight. *Radiology* 2004;230:142–150.
24. Lee CH, Goo JM, Kyongtae KT, et al. CTA contrast enhancement of the aorta and pulmonary artery: the effect of saline chase injected at two different rates in a canine experimental model. *Invest Radiol* 2007;42:486–490.
25. Claves JL, Wise SW, Hopper KD, et al. Evaluation of various contrast densities in the diagnosis of carotid stenosis by CT angiography. *AJR Am J Roentgenol* 1997;169:569–573.
26. Suzuki S, Furui S, Kaminaga T, et al. Measurement of vascular diameter in vitro by automated software for CT angiography. *AJR Am J Roentgenol* 2004;182:1313–1317.
27. Johnson JA, Phalen DN, Kondik VH, et al. Atherosclerosis in psittacine birds, in *Proceedings*. Assoc Avian Vet Conf 1992;87–93.
28. St Leger J. Avian atherosclerosis. In: Fowler ME, Miller RE, eds. *Zoo and wild animal medicine, current therapy VI*. St Louis: WB Saunders Co, 2007;200–205.